Characterization of Defatted Soy Flour and Elastomer Composites

L. Jong

United States Department of Agriculture, National Center for Agricultural Utilization Research, Agricultural Research Service, 1815 North University Street, Peoria, Illinois 61604

Received 17 December 2004; accepted 4 February 2005
DOI 10.1002/app.22094
Published online in Wiley InterScience (www.interscience.wiley.com).

ABSTRACT: Defatted soy flour (DSF) is an abundant renewable commodity and is more economically favorable then soy protein isolate or soy protein concentrate. DSF contains soy protein, soy carbohydrate, and soy whey. The aqueous dispersion of DSF was blended with styrene-butadiene latex to form elastomer composites. The inclusion of soy carbohydrate increased the tensile stress in the small strain region, but reduced the elongation at break. The shear elastic modulus of the composites showed an increase in the small strain region, consistent with its stress-strain behavior. The inclusion of soy carbohydrate and soy whey also improved the recovery behavior in the nonlinear region. At small strain, the shear elastic modulus of 30% filled composites at 140°C was about 500 times higher than that of the unfilled elastomer, indicating a significant reinforcement effect generated by DSF. Compared with soy protein isolate (SPI), the stress softening effect and recovery behavior under dynamic strain indicate the addition of soy carbohydrate and soy whey may have increased the filler-rubber interaction. In general, the DSF composites gave better mechanical properties compared with the protein composites. © 2005 Wiley Periodicals, Inc.* J Appl Polym Sci 98: 353–361, 2005

Key words: composites; defatted soy flour; elastomers; mechanical properties; reinforcement

INTRODUCTION

Defatted soy flour (DSF) is a soy product after soybean oil is removed from soybean flakes. It is an abundant and inexpensive renewable commodity. The composition of defatted soy flour includes soy protein, soy carbohydrate (insoluble carbohydrate), and soy whey (soluble carbohydrate).[1] DSF also has the lowest cost compared with soy protein concentrate (SPC) and soy protein isolate (SPI) because it is the raw material for the production of those soy products. Many investigations in recent years reported the modulus enhancement of rubbers by natural materials, for example, oil palm wood,[2] crab shell chitin,[3] and bamboo fiber.[4] From the perspective of renewable materials and environmental reasons, soy protein and other soybean products have been investigated as a component in plastic and adhesive composites,[5–9] but have been rarely investigated as a reinforcement component in elastomers. Dry soy protein is a rigid material and has a shear elastic modulus of ~ 2 GPa under ambient conditions.[6] Dry DSF is also a rigid material. Because the high rigidity of a reinforcement phase is one of the requirements in rubber reinforcement, dry DSF is therefore a possible candidate for this application. Attempts to use protein in rubber latex can be traced back to the 1930s. A few patents[10–12] had claimed the use of protein in rubber composites. For example, Lehmann and coworkers had demonstrated the use of casein (milk protein) in natural rubber latex to achieve approximately a 4-fold increase in the modulus.[12] Protein as an additive in rubber materials also has been claimed to improve the antiskid resistance of winter tread tires.[13–15] In rubber reinforcement, factors such as aggregate structure, effective filler volume fraction, filler-rubber interaction, and elastic modulus of filler clusters have important impact on the modulus of rubber composites.[16]

Previously, globular soy protein aggregates were used to reinforce styrene-butadiene rubber and indicated a significant reinforcement effect in the small strain region.[17] For many applications, DSF is economically more favorable than soy protein concentrate or soy protein isolate. The objective of this investigation is to compare its reinforcement effect with soy protein isolate (SPI) to obtain some information on the effect of soy carbohydrate and soy whey. In this study, the rubber matrix chosen is a styrene-butadiene (SB) rub-

Correspondence to: L. Jong (jongl@ncaur.usda.gov).

Names are necessary to factually report on available data; however, the USDA neither guarantees nor warrants the standard of the product, and the use of the name by USDA implies no approval of the product to the exclusion of others that may also be suitable.

Journal of Applied Polymer Science, Vol. 98, 353–361 (2005)

ber with a small amount of carboxylic acid containing monomer units because previous studies have indicated the importance of interaction between filler and matrix.[18] Soy protein contains a significant amount of carboxylic acid and substituted amine group.[19] Soy carbohydrate and soy whey are also capable of interacting with carboxylic functional groups in an SB matrix through hydrogen bonding and ionic interaction. Structurally, soy protein is a globular protein and its aggregate is similar to colloidal aggregates, but soy carbohydrate and soy whey are nonglobular and film-forming materials. For practical applications, the issue of moisture sensitivity in some applications is always associated with natural materials, but it may be improved through product formulation and/or selective applications. For example, it may be used as a component in multi-layered structures, in coated objects, in elevated temperature applications, or as a rubber part in greasy/oily environments where the moisture effect is minimum.

The rubber composites investigated here are prepared by casting films from the dispersion of DSF and carboxylated styrene-butadiene latex. To give some background on the rubber matrix of this composite, the properties of carboxylated SB rubber will be described briefly. Carboxylated SB rubber is classified as an ion-containing polymer where the viscoelastic properties are affected by molecular weight, degree of crosslinking, glass transition temperature (T_g), copolymer composition, number of ionic functional groups, size of ionic aggregation, degree of neutralization, and size of the neutralizing ions.[20,21] Previous studies also have shown honeycomb-like structures in the film of carboxylated latices due to higher concentration of carboxylic acid groups on the particle surface.[22] Mechanically, the elastic modulus of base rubber is not significant when compared with the modulus of filler network in highly filled elastomeric composites.[18]

EXPERIMENTAL

Materials

The DSF used in this research was a spray dried powder (Nutrisoy 7B, Archer Daniels Midland Company, Decatur, IL). The soy protein used as a comparison is a slightly enzyme hydrolyzed soy protein isolate (PRO-FAM 781, Archer Daniels Midland Company). Sodium hydroxide, used to adjust pH, was ACS grade. The carboxylated styrene-butadiene (SB) latex was a random copolymer of styrene, butadiene, and a small amount of carboxylic acid containing monomers (CP 620NA, Dow Chemical Company, Midland, MI.). The glass transition temperature of carboxylated SB Latex is $\sim$ 10°C determined by differential scanning calorimetry. Styrene/butadiene ratio estimated from the glass transition temperatures of a series of commercially available carboxylated styrene butadiene was approximately 65/35. The dried latex is not known to be soluble in any solvent or a combination of solvents. The latex received had $\sim$ 50% solids and a pH $\sim$ 6. The volume weighted mean particle size of the latex was $\sim$ 0.18 μm.

Preparation of elastomer composites

DSF was first dispersed in water and the pH was adjusted to 9 with sodium hydroxide and then mixed with SB latex already adjusted to pH 9. The composites of DSF and carboxylated SB latex were prepared by first casting an emulsion of the blend onto an aluminum mold covered with Teflon release sheet (BYTAC from Saint-Gobain Performance Plastics) and then allowing it to dry at 75°C for 72 h. After drying at low temperature, the samples were removed from the mold and annealed at 110°C and 140°C for 24 h, respectively. Dry composites containing 10 to 30% by weight of DSF were prepared. The film of 100% carboxylated SB rubber was prepared by adjusting the pH of latex to 9 and drying under the same conditions as that of the DSF/SB composites. The composites of soy protein isolate (Soy/SB) were also prepared by the same procedure. The dried carboxylated SBR film contained less than 0.3% moisture and the dried DSF/SB and Soy/SB composites had moisture contents less than 0.8% as measured by halogen moisture analyzer (Mettler Toledo HR73) at 105°C for 60 min. For the 100% DSF and soy protein, torsion bars could not be made by the casting method. The freeze-dried powder was compression molded at 44 MPa and 140°C for 2 h. After compression molding, the samples were relaxed at 140°C for 24 h.

Scanning electron microscopy

The morphology of DSF and soy protein aggregates was examined by scanning electron microscopy (SEM) using a JEOL JSM-6400V instrument. Images of these soy products were obtained by casting onto an aluminum substrate a dilute dispersion of DSF or protein at pH 9 and at a concentration of 0.004%. The samples on aluminum stubs were then coated with Au-Pd and examined under vacuum at ambient temperature.

Particle size measurements

The mean particle size and distribution of DSF and protein aggregates were measured by using a Horiba LA-930 laser scattering particle size analyzer with red light wavelength of 632.8 nm and blue light wavelength of 405 nm. The measurement is based on Mie scattering theory and has a measurement range of 0.02 to 2000 μm. The volume weighted mean diameter of 0.17 μm was obtained for the styrene-butadiene latex

and was in good agreement with the particle size value of 0.18 μm supplied by Dow Chemical Company.

Stress-Strain measurements

The stress-strain measurements were conducted by using an Instron 4201 (Instron Corporation, Canton, MA) with Instron Series IX software control. All samples were measured in dry state without conditioning and the sample size was approximately 12.5 × 60 × 3 mm. All measurements were conducted at a speed of 50 mm/min under the ambient condition of 23°C.

Dynamic mechanical measurements

For all strain sweep experiments, the oscillatory storage and loss moduli, G′(ω) and G″(ω), were measured using a Rheometric ARES-LSM rheometer with a torsional rectangular geometry. A rectangular sample with dimensions of approximately 12.5 × 20 × 3 mm was inserted between the top and bottom grips. The gap between the fixtures was 5 to 6 mm to achieve a strain of ~ 15%. A sample length shorter than 5 mm is not desirable because of the shape change from the clamping at both ends of the sample. The frequency used in the measurements was 1 Hz. The oscillatory storage and loss moduli were measured over a strain range of approximately 0.007 to 15%. The actual strain sweep range was limited by sample geometry and motor compliance at large strain, and transducer sensitivity at small strain. Although harmonics in the displacement signal may be expected in nonlinear material, a previous study[23] indicated that the harmonics are not significant if the shearing does not exceed 100%. Each sample was conditioned at 80°C or 140°C for 30 min and then subjected to 8 cycles of dynamic strain sweep to study the stress softening effect.

Temperature ramp experiments were conducted using torsion rectangular geometry with a heating rate of 1°C/min and a temperature range from −40 to 140°C. The soak time at each temperature after ramp was 15 s and the measurement duration at each temperature was 30 s. When using torsion rectangular geometry, torsional bars with dimensions of approximately 40 × 12.5 × 3 mm were mounted in the torsion rectangular fixtures and the dynamic mechanical measurements were conducted at a frequency of 0.16 Hz (1 rad/s) and a strain of 0.05%.

RESULTS AND DISCUSSION

Stress-Strain behavior

Figure 1 shows the stress-strain behavior of DSF and protein composites at ambient conditions. Compared with soy protein at the same weight fraction, DSF

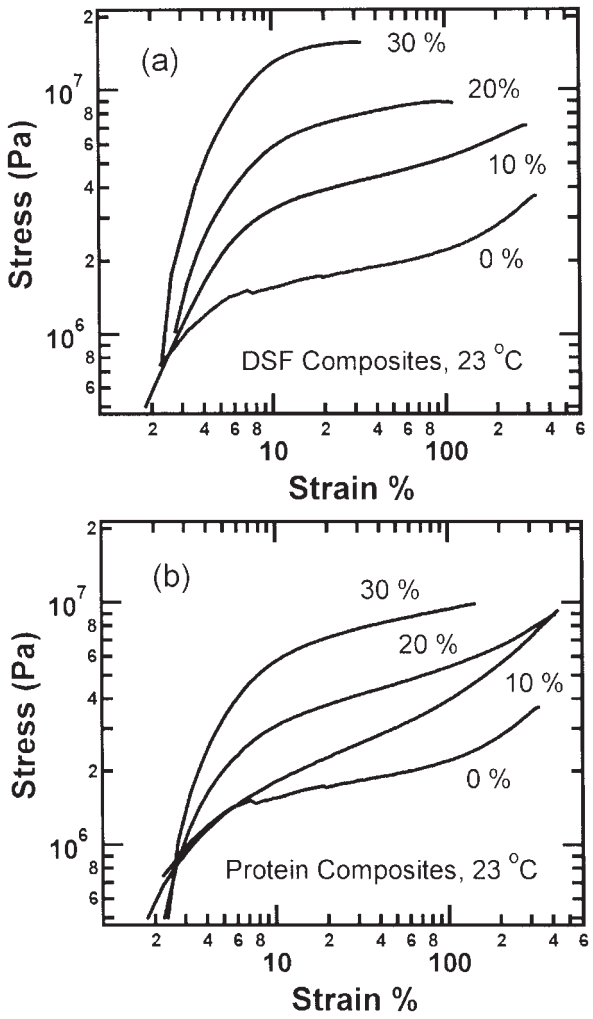

Figure 1 Stress-strain behaviors at ambient conditions: (A) DSF composites, (B) Soy protein composites.

composites showed a higher modulus in the small strain region, but the elongation at break was also reduced. Comparing the tensile stress at break for both composites, the DSF composites exhibited a slightly lower value for the 10% composite and a similar value for the 20% composite, but exhibited a higher value for the 30% composite. Comparing the toughness estimated from the area under the stress-strain curve, the trend is similar to the tensile stress at break because a lower elongation at break compensates the higher tensile stress of the DSF composites in the lower strain region. This indicates the inclusion of soy carbohydrate and soy whey does not improve the ultimate strength of the composites containing less than 20% of fillers, but it significantly increases the composite strength at the lower strain region. This also indicates the effect of soy carbohydrate significantly changes the rigidity of the SB rubber and gradually exhibits a plastic instead of rubber like behavior as the DSF concentration increases. These behaviors were also reported for DSF/polyurethane compos-

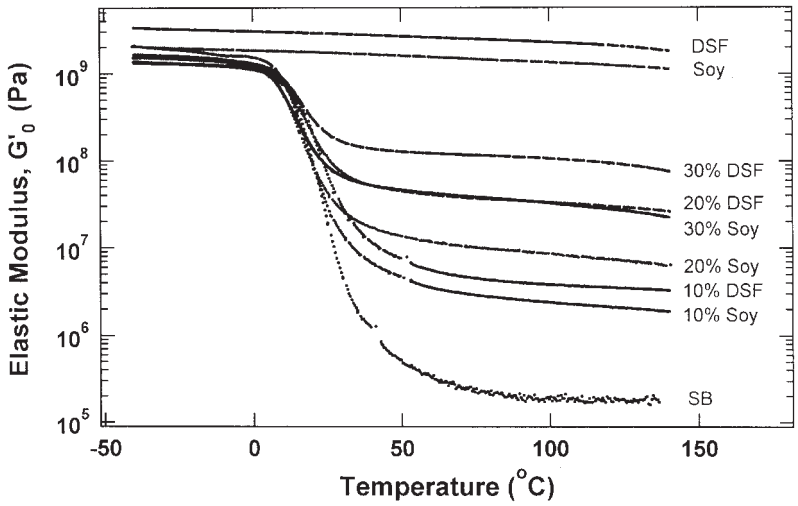

Figure 2 Storage moduli of DSF/SB and Soy/SB composites. The weight fraction of filler is indicated at the end of each curve.

ites.[24] The low strain behaviors are consistent with that measured by the dynamic mechanical method and will be investigated further in the following sections. In general, the stress-strain behaviors indicate the filler loading in these soy composites is an important parameter to adjust to obtain different material characteristics for different applications.

Shear elastic modulus

As shown in Figure 2, the addition of DSF dispersion into styrene-butadiene rubber caused a significant reinforcement effect in the rubber plateau region. The reinforcement effect was proportional to the DSF content. Comparing DSF and soy protein filled composites at 20 and 30% concentrations, the difference in the moduli was significant between these two composites. The elastic moduli of 100% DSF and soy protein are also shown in the top portion of Figure 2. DSF prepared under the same condition as that of soy protein exhibited a higher elastic modulus. The higher rigidity of DSF accounts for part of the reason that elastic moduli of its composites were higher than that of soy protein in the small strain region. Other factors include the difference in filler-rubber interaction in the stress softening effect that will be discussed later.

A better understanding can be had by examining the SEM pictures of both DSF and soy protein in Figure 3. Figure 3(a) shows soy protein aggregates are embedded in the film-like soy carbohydrate and soy whey. Compared with Figure 3(b), it is clear that soy protein aggregates have a globular structure, while soy carbohydrate and soy whey have a film-like structure. The white protein globules in Figure 3(a) have about the same size ($\sim$ 0.3 μm) as in Figure 3(b). However, the number average dry size of DSF estimated from Figure 4 is about 6 μm, which is much greater than the size of protein globules. This indicates the wet particles of DSF are composed of both protein globules and soy carbohydrate. Figure 3(c) shows the morphology of soy protein concentrate (SPC), where the water-soluble soy whey has been removed. The size of soy protein globules covered by soy carbohydrate in SPC appears to be larger than that in DSF. To examine if soy carbohydrate could behave as an adhesive network to bridge the soy protein aggregates, aggregate size measurements were conducted in water under ultrasonic dispersion. The size distribution curves are shown in Figure 4. After both DSF and soy protein dispersion were subjected to the same ultrasonic dispersion for the same period, soy protein aggregates were significantly reduced in size, whereas the DSF only changed slightly. This indicates the protein embedded DSF aggregates are strong and the soy carbohydrate is capable of holding the protein aggregates together. This effect is also expected to be operating in the composites in terms of enhancing the filler network strength in the small strain region. The particle size data also indicates DSF dispersion is dominated by the large particles in terms of volume or weight, but it also contains a large number of smaller particles [Fig. 4(b)]. Because the weight or volume fraction of soy products changes the mechanical properties of the composites significantly, the larger particle aggregates are therefore the dominating factor for the rubber reinforcement. However, in elastomers with the same filler fraction, it is known that smaller particles should have a greater reinforcement effect than larger particles because their effective volume fractions are larger due to a greater surface area and a greater amount of immobilized rubber polymers.[16] The fact that DSF composites are stronger than protein composites in the small strain region indicates the

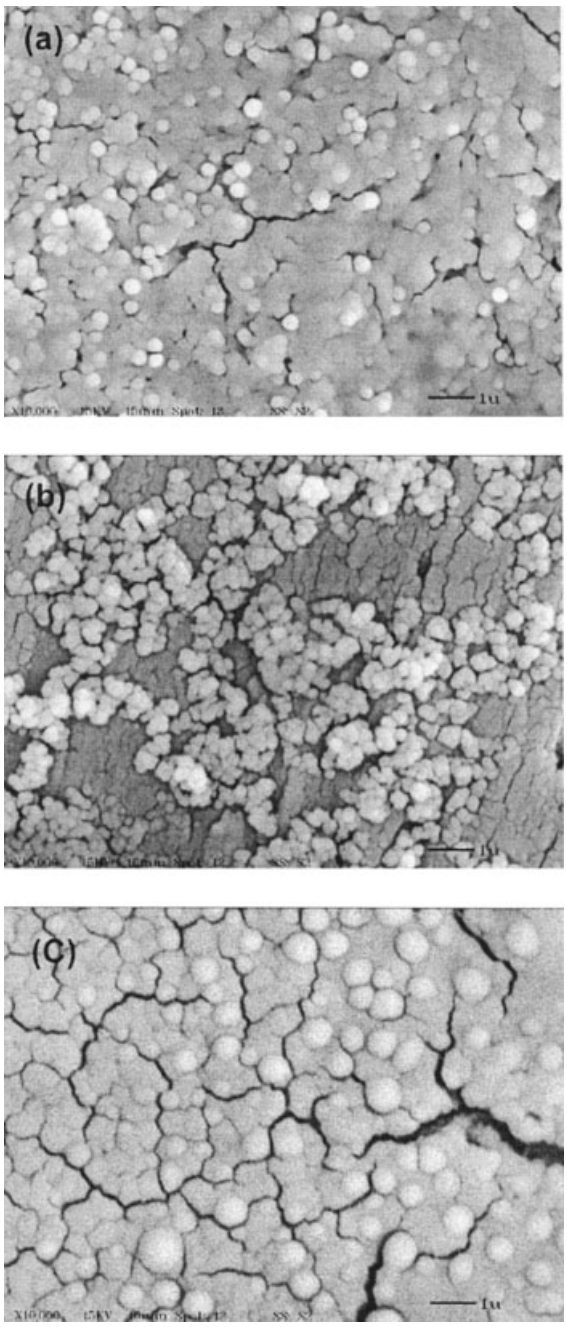

Figure 3 (A) The DSF film on an aluminum substrate showing the soy protein aggregates are embedded in the soy carbohydrate film. (B) Soy protein aggregates (SPI) on a gray mottled aluminum substrate. (C) SPC film. The scale of the black bar located at the right bottom corner is 1 μm.

filler network strength is a dominating factor for these composites at small strain.

In the rubber plateau region, the elastic moduli of DSF and soy protein composites were plotted against the weight and volume fraction of fillers (Fig. 5). The DSF generated a more significant reinforcement effect than the soy protein in the concentration range studied, and the difference between the moduli of DSF and those of the soy protein was similar in all concentrations. From the slope of elastic modulus versus volume fraction, it was observed that the modulus of DSF composites increased with filler concentration similar to that of the protein composites. The slope of plots in Figure 5(b) is $\sim$ 2.7 for DSF composites and is $\sim$ 2.6 for soy protein composites. Overall, DSF shows an improvement over protein in the reinforcement of elastomers, but has a much lower cost than protein.

Stress softening effect

The stress softening effect occurs in most filled elastomers. In these systems, the stress required to deform the filled rubber at a given elongation is reduced during the second cycle of deformation. The effect is also called the Mullin effect for his extensive studies[25,26] on this phenomenon. The stress softening effect is generally considered to be caused by filler related structures and therefore can yield some insight into the filler structures.[18] The stress softening effect of 100% styrene-butadiene (SB) rubber, 30% DSF filled styrene-butadiene rubber composite (30/70 DSF/SB), and 30% soy protein filled styrene-butadiene rubber composite (30/70 Soy/SB) is shown in Figure 6. Similar to carbon black or silica filled elastomers,[18] the

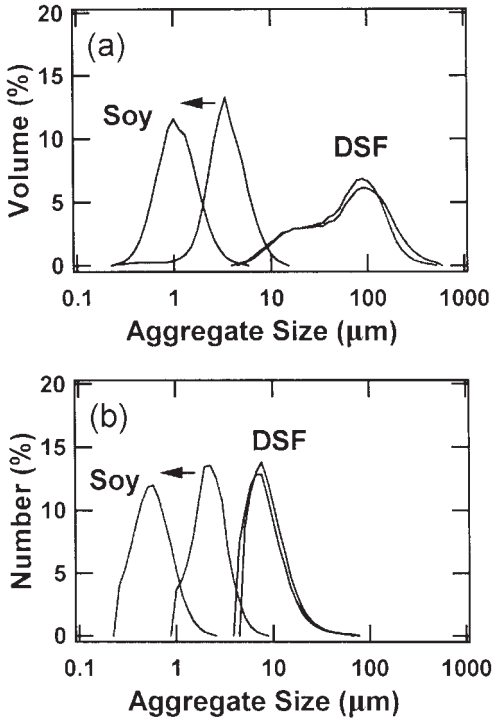

Figure 4 The measurements of volume (A) and number (B) weighted aggregate size in water. Both DSF and soy protein aggregates were subjected to 1 hour of ultrasonic dispersion. Aggregate size of the soy protein is significantly reduced and the size distribution curve is shifted to the left, whereas that of the DSF only changes slightly.

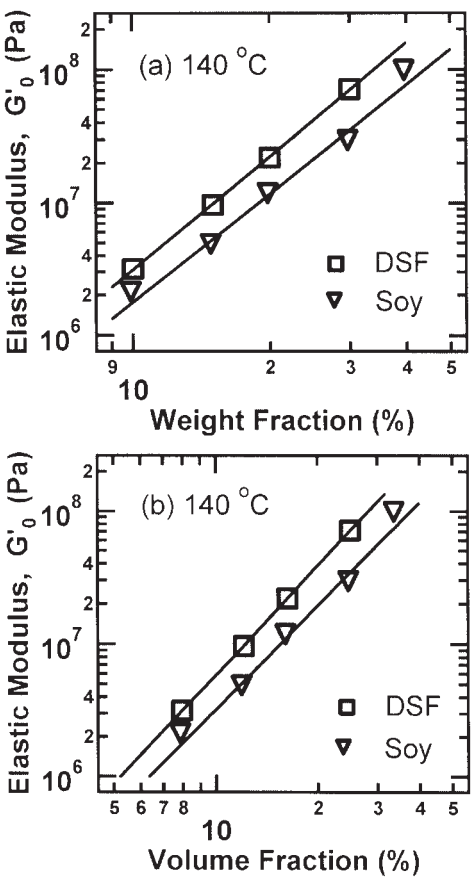

Figure 5 Elastic moduli of DSF and Soy composites at small strain region plotted against weight (A) and volume (B) fractions. The measurements were conducted at 0.16 Hz and 140°C.

DSF and soy protein composites show a significant reduction in the shear elastic modulus after the first strain cycle. At 80°C, the strain sweep curves for both 30/70 DSF/SB and Soy/SB composites become more reproducible after 4 cycles of dynamic strain. 100% styrene-butadiene rubber also shows a stress softening effect, but its contribution to the stress softening effect of the composites is not significant. This is evident by comparing the differences between the first and the eighth strain cycles of shear elastic modulus in Figures 6a and b. The contribution of the stress softening effect from the rubber is less than 0.5% in the stress softening effect of 30/70 DSF/SB or 30/70 Soy/SB composite. The stress softening effect in DSF/rubber composites is caused mostly by the contribution from DSF related structures, such as the DSF network and DSF-rubber interactions. The increasing magnitude of strain (deformation) in the first 4 strain cycles apparently causes the filler network to break down and possibly the polymer chains to detach from the filler aggregates. In this aspect, the current DSF/rubber composites are not very different from the well-known carbon black filled rubber composites. After 4 strain cycles, filler related network structures can be broken and reformed, and this is an indication of reaching an equilibrium condition. The mechanism of agglomeration and de-agglomeration of fillers is based on the elasticity of a filler immobilized rubber network and not on the elasticity of a filler network, because the rigid filler network is broken when it is deformed beyond the small strain region. The recovery of the deformed

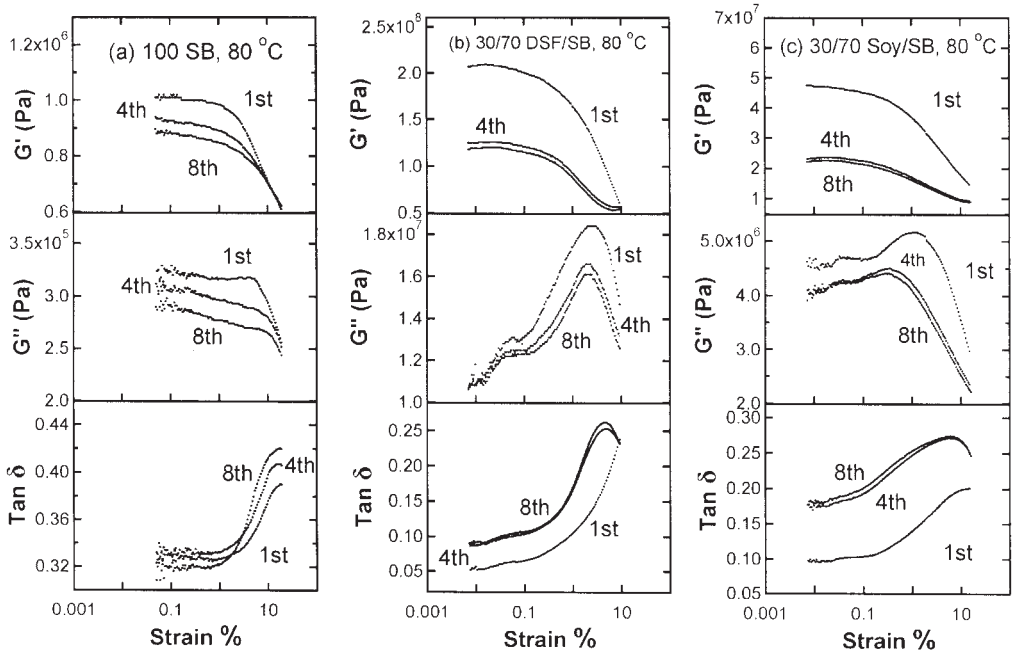

Figure 6 Strain sweep experiments: (A) 100% SB at 80°C, (B) 30/70 DSF/SB composite at 80°C, and (C) 30/70 Soy/SB composite at 80°C.

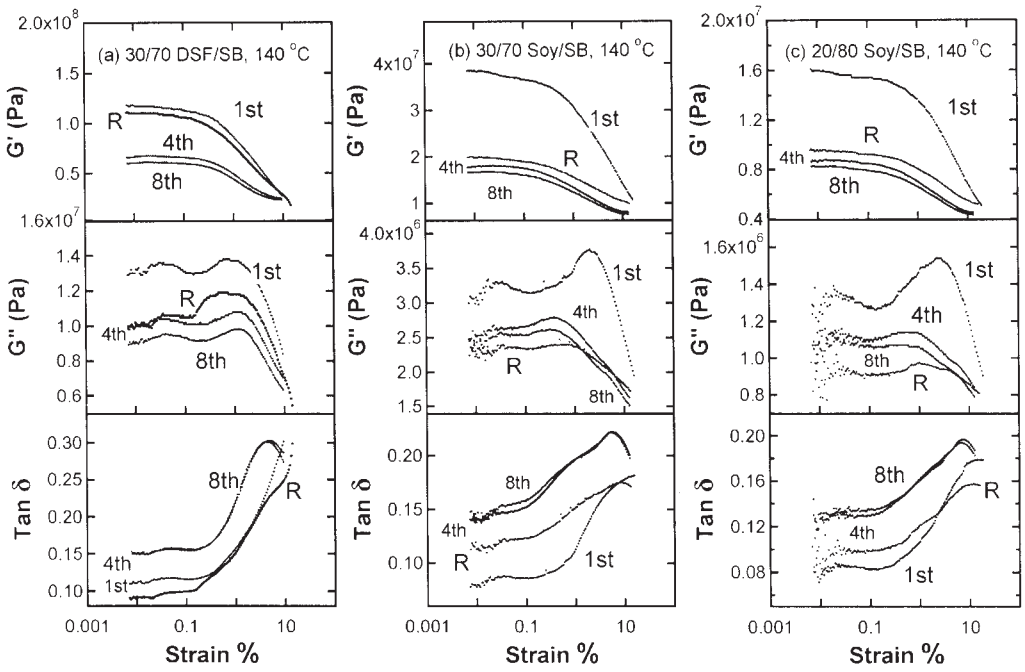

Figure 7 Strain sweep experiments at 140°C: (A) 30/70 DSF/SB composite, (B) 30/70 Soy/SB composite, and (C) 20/80 Soy/SB composite. R indicates the recovery curve after the samples are conditioned at 140°C for 24 h.

composite therefore comes entirely from the elasticity of the filler immobilized rubber shell around the fillers. The network structure of immobilized rubber shell around the filler network is a reflection of filler structure and therefore can be characterized by the filler structure. The immobilized rubber network is analogous to a rubber with a higher crosslinking density and therefore has a better memory to return to its original shape when compared to a rubber with a lower crosslinking density. A stronger interaction between filler and rubber matrix has been shown to be effective in improving modulus recovery.[27]

For loss modulus under cyclic strain, the energy dissipation process of protein composites became less pronounced and the maximum was shifted to lower strain amplitudes. The structure responsible for the energy dissipation process is obviously reduced after the first 4 cycles. However, the loss maximum of the DSF composite did not shift significantly along the strain axis and its magnitude did not decrease as much as that of protein composites. In the first strain cycle, the ratio of the loss modulus at maximum to the loss modulus value at 0.01% strain is ~ 1.7 for the DSF composite [Fig. 6(b)] and ~ 1.1 for the protein composite [Fig. 6(c)]. Comparing the DSF composite with the protein composite, the magnitude of loss maximum in the protein composite is not as pronounced as that in the DSF composite, indicating the DSF composite has a stronger structure.

The magnitudes of shifting in the position of loss maxima in Figures 6(b) and c are also different. At 80°C, the Soy/SB composite in Figure 6(c) exhibited a loss maximum at 1.2% strain in the first cycle, whereas the DSF/SB composite in Figure 6(b) had a loss maximum at 2.4% strain in the first cycle. In the eighth cycle, the loss maximum of the protein composite occurred at 0.3% strain and that of the DSF composite was at 2.1% strain. A greater shifting of loss maximum towards the lower strain at the eighth cycle in the protein composite may indicate the protein related network structure is slower to recover than that of the DSF composite within the same period. At 140°C, the same phenomenon was again observed in Figure 7. This observation is also consistent with the recovery curves shown in Figure 7, where the DSF composite recovered 90% of its G'_0, the 30/70 Soy/SB composite recovered 52% of its G'_0, and the 20/80 Soy/SB composite recovered 59% of its G'_0. This indicates the DSF composite has a better modulus recovery than the protein composite under the same condition. This is not an effect of filler volume fraction. The volume fraction of DSF in the 30/70 DSF/SB composite is smaller than that of 30/70 Soy/SB composite because the density of DSF (1.41 g/cm3) is greater than that of soy protein (1.3 g/cm^3). The 20/80 Soy/SB composite [Fig. 7(c)] has a smaller filler volume fraction than the 30/70 DSF/SB composite, but its loss modulus and recovery curve [Fig. 7(c)] show the same tendency as that of the 30/70 Soy/SB composite [Fig. 7(b)]. Previously, it was shown that a stronger filler-rubber interaction could yield a better recovery behavior.[27] Therefore, a stronger DSF-rubber interaction in the DSF

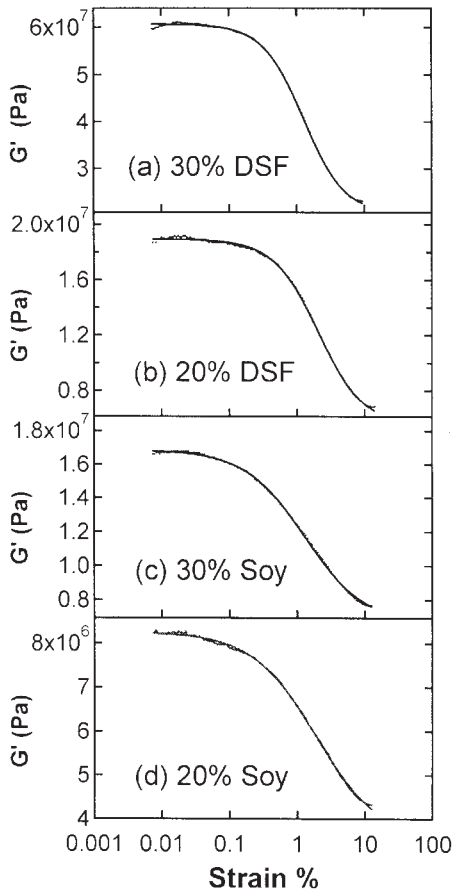

Figure 8 The 8th cycle of strain sweep experiments at 140°C and 1 Hz: (A) 30/70 DSF/SB composite, (B) 20/80 DSF/SB composite, (C) 30/70 Soy/SB composite, and (D) 20/80 Soy/SB composite. Solid lines are the fit from the Kraus model.

composites compared with that of the soy protein may explain these recovery behaviors.

Elasticity of DSF related rubber structures

The stress softening data can also be analyzed further to obtain more information on the reinforcement effect of DSF. The shear elastic moduli of filled elastomers with 20 and 30% of DSF and soy protein aggregates are shown in Figure 8. The data shown is the eighth cycle of strain sweep. The resulting modulus-strain spectra are similar to that of carbon black.[18] The reduction of shear elastic modulus with increasing strain is a familiar phenomenon, reported by Payne on carbon black filled rubbers in the early 1960s. Later, Kraus[28] proposed a phenomenological model based on Payne's idea of filler networking. The model is based on the aggregation and de-aggregation of carbon black agglomerates. In this model, the carbon black contacts are continuously broken and reformed under a periodic sinusoidal strain. Based on this kinetic aggregate forming and breaking mechanism at equilibrium, elastic modulus was expressed as follows:

$$\frac{G'(\gamma) - G'_\infty}{G'_0 - G'_\infty} = \frac{1}{1 + (\gamma/\gamma_c)^{2m}} \quad (1)$$

where G'_∞ is equal to $G'(\gamma)$ at very large strain, G'_0 is equal to $G'(\gamma)$ at very small strain, γ_c is a characteristic strain where $G'_0 - G'_\infty$ is reduced to half of its zero-strain value, and m is a fitting parameter related to filler aggregate structures. Equation (1) has been shown to describe the behavior of $G'(\gamma)$ in carbon black filled rubber reasonably.[16] The loss modulus and loss tangent, however, do not have a good agreement with experiments,[29] mainly due to uncertainty in the formulation of the loss mechanism. Recently, Huber and colleagues also modeled the Payne effect and gave a similar expression as the Kraus model, but with a physical interpretation of the fitting parameter m in the Kraus model. Based on the cluster-cluster aggregation (CCA) model, Huber and colleagues[30] obtained $m = 1 / (C - d_f + 2)$, where C is a connectivity exponent related to the minimum path along the cluster structure and d_f is the fractal dimension of clusters. Therefore, the fitting parameter m has a physical meaning related to filler structures or filler immobilized rubber structures (a reflection of filler structure). The fractal dimension of fractal-like protein clusters can be estimated from the slope in Figure 5 by using the strong link model[31] because the protein aggregates form a network above the percolation threshold.[32] The strong link model indicates $\log G'_0 \sim (3 + C)/(3 - d_f) \log \phi$, where ϕ is the volume fraction of particles and C and d_f have been defined previously. C takes a value from 1 to d_f.[31] For soy protein aggregates, d_f is estimated to be 1.35–1.48. The parameter m can be estimated from the fractal dimension of soy protein aggregates and is approximately in the range 0.47–0.65. The agreement between the estimation and the best fit of experimental data shown in Figure 8 and Table I is reasonable and is similar to that of carbon black composites, $m = 0.5$–0.6.[16,33] For DSF composites, the estimated fractal dimension from Figure 5 is 1.39–1.53 and the parameter m is estimated to be 0.49–0.74. The estimated range for parameter m is somewhat large due to uncertainty in the parameter C. Furthermore, the DSF structure consisting of soy carbohydrate and soy whey embedded with protein aggregates may no longer fit the definition of a particle aggregate. Therefore, it may not be appropriate to use a fractal-like description for the DSF composites. However, an empirical fit is provided to demonstrate the difference in the curve shapes (Fig. 8) between the DSF and protein composites. In general, the fitting parameter $m \approx 0.7$ for DSF composites is apparently different from that of soy

TABLE I
Fit Parameters of Shear Elastic Modulus[1]

Composition	Best fit[2] m		γ_c (%)	G'_0 (MPa)	G'_∞ (MPa)
DSF/SB	4th cycle	8th cycle	8th cycle	8th cycle	8th cycle
20/80	0.73 ± 0.02	0.66 ± 0.02	2.05 ± 0.03	18.9 ± 0.5	5.59 ± 0.23
30/70	0.70 ± 0.02	0.72 ± 0.02	1.27 ± 0.03	60.6 ± 0.1	20.5 ± 0.4
Soy/SB					
20/80	0.51 ± 0.02	0.46 ± 0.02	1.88 ± 0.13	8.25 ± 0.03	3.53 ± 0.13
30/70	0.51 ± 0.02	0.46 ± 0.02	1.39 ± 0.07	16.9 ± 0.06	6.2 ± 0.2

[1] Measured at 140°C.
[2] Best fit of shear elastic modulus vs. strain with the Kraus Model.

protein composites and reflects a difference in their structures shown in Figures 3a and b.

CONCLUSIONS

DSF was incorporated at different levels into carboxylated SB elastomers. The inclusion of soy carbohydrate increased the tensile stress in the small strain region, but reduced the elongation at break. Both tensile strength at break and toughness were increased when the DSF content is greater than 20%, but remained the same or less when the DSF content is less than 20%. In the rubber plateau region, a very significant increase in the shear elastic modulus of dry composites was observed when compared with that of 100% carboxylated SB elastomer. The observed significant reinforcement effect was studied by dynamic temperature sweep experiments and compared with that of soy protein isolate. At the same weight fraction of fillers, DSF exhibited a higher reinforcement effect than that of soy protein in the rubber plateau region. The composites were also studied by using dynamic strain sweep experiments to understand the filler related structures. Both DSF and soy protein structures exhibited similar behavior in terms of reversible structure breakdown after 4 cycles of dynamic shear strain. The DSF composites exhibited a better recovery behavior after 8 cycles of dynamic strain, indicating a stronger filler-rubber interaction. The Payne effect of DSF and protein composites at 140°C was interpreted using the Kraus model. The fitting parameter m for DSF composites was found to be different from that of soy protein composites. This study indicates the use of DSF in rubber composites is a better option than soy protein in terms of both mechanical properties and cost.

The author thanks Dr. A. R. Thompson for scanning electron microscopy and A. J. Thomas for Instron measurements.

References

1. Carter, C. M; Cravens, W. W.; Horan, F. E.; Lewis, C. J.; Mattil, K. F.; Williams, L. D. In Protein Resources and Technology; Milnre, M.; Scrimshaw, N. S.; Wang, D. I. C., Eds.; AVI Publishing: Westport, CT, 1978; Chapter 17.
2. Ismail, H.; Jaffri, R. M.; Rozman, H. D. J Elastomers Plast 2003, 35, 181.
3. Nair, K. G.; Dufresne, A. Biomacromolecules 2003, 4, 666.
4. Ismail, H.; Shuhelmy, S.; Edyham, M. R. Eur Polym Mater 2001, 38, 39.
5. Wang, C.; Carriere, C. J. U.S. Pat. 6,310,136 B1 (2001).
6. Wang, S.; Sue, H. J.; Jane, J. J. M. S-Pure Appl Chem 1996, A33, 557.
7. Paetau, L.; Chen, C.; Jane, J. Ind Eng Chem Res 1994, 33, 1821.
8. Mo, X.; Sun, X. S.; Wang, Y. J Appl Polym Sci 1999, 73, 2595.
9. Wu, Q.; Zhand, L. Ind Eng Chem Res 2001, 40, 1879.
10. Coughlin, E. T. A. U.S. Pat. 2,056,958 (1936).
11. Isaacs, M. R. U.S. Pat. 2,127,298 (1938).
12. Lehmann, R. L.; Petusseau, B. J.; Pinazzi, C. P. U.S. Pat. 2,931,845 (1960).
13. Fuetterer, C. T. U.S. Pat. 3,113,605 (1963).
14. Beckmann, O.; Teves, R.; Loreth, W. Ger Offen DE 19622169 A1 19961212 (1996).
15. Recker, C. Eur Pat Appl EP 1234852 A1 20020828 (2002).
16. Heinrich, G.; Kluppel, M. Adv Polym Sci 2002, 160, 1.
17. Jong, L. Compos A 2005, 36, 675.
18. Wang, M. J. Rubber Chem Technol 1998, 71, 520.
19. Garcia, M. C.; Torre, M.; Marina, M. L.; Laborda, F. Crit Rev Food Sci Nutr 1997, 37, 361.
20. Richard, J. Polymer 1992, 33, 562.
21. Zosel, A.; Ley, G. Macromolecules 1993, 26, 2222.
22. Kan, C. S.; Blackson, J. H. Macromolecules 1996, 29, 6853.
23. Chazeau, L.; Brown, J. D.; Yanyo, L. C; Sternstein, S. S. Polym Compos 2000, 21, 202.
24. Chen, Y.; Zhang, L.; Du, L. Ind Eng Chem Res 2003, 42, 6786.
25. Mullins, L. J Rubber Res 1947, 16, 275.
26. Mullins, L. Phys Colloid Chem 1950, 54, 239.
27. Zhu, A.; Sternstein, S. S. Compos Sci Technol 2003, 63, 1113.
28. Kraus, G.; J Appl Polym Sci, Appl Polym Symp 1984, 39, 75.
29. Ulmer, J. D. Rubber Chem Technol 1995, 69, 15.
30. Huber, G.; Vilgis, T. A. Kautsch Gummi Kunstst 1999, 52, 102.
31. Shih, W.; Shih, W. Y.; Kim, S.; Liu, J.; Aksay, I. A. Phys Rev A 1990, 42, 4772.
32. Jong, L. Polym Mater Sci Eng 2004, 90, 769.
33. Heinrich, G.; Vilgis, T. A. Macromol Chem Phys, Macromol Symp 1995, 93, 253.